Fiber-Reinforced Polymer Reinforcement for Concrete Structures

10th International Symposium

Editors:
Rajan Sen
Rudolf Seracino
Carol Shield
Will Gold

American Concrete Institute®

SP-275

ACI Design Guide for Flexural and Shear Strengthening of URM Walls with FRP Systems

J. Gustavo Tumialan, William J. Gold, Nestore Galati, and Andrea Prota

Synopsis: The American Concrete Institute (ACI) Committee 440 has recently published a design guide for strengthening of masonry with FRP systems. This paper summarizes and provides comments on the design protocols recommended by ACI 440 for flexural and shear strengthening with FRP systems of unreinforced masonry wall (URM). The development of the design protocols were based on calibration of bond reduction factors derived by a database of test results. This paper presents the rationale behind this approach, the calibration procedure, and its implementation in design protocols for flexural and shear strengthening of URM walls.

Keywords: Design, Fiber Reinforced Polymer (FRP), Flexure, Shear, Strengthening, Unreinforced Masonry

J. Gustavo Tumialan, ACI Member, is a Senior Project Manager at Simpson Gumpertz and Heger, Inc. in Boston, MA. He received his B.S. in Civil Engineering from Pontificia Universidad Catolica del Peru; and MSc., and Ph.D. from the Missouri University of Science and Technology. He specializes in the investigation, evaluation, and rehabilitation of structures. He is a member of ACI Committees 437, 440, and 562. He was a member of the Task Group that prepared ACI 440.7R-10.

William J. Gold, ACI Member, is the Engineering Services Manager for BASF Corporation - Building Systems in Cleveland, OH. He has over 12 years of experience in the use of advanced composite materials in the construction industry. He holds a Bachelor's degree in Architectural Engineering from the University of Kansas. He is the current Secretary of ACI Committee 440 and was a member of the Task Group that prepared ACI 440.7R-10.

Nestore Galati, ACI Member, is a Senior Design Engineer at the Structural Group, Inc. in Elkridge, MD. He received his B.S. and Ph.D. from University of Lecce in Italy, and MSc. from the Missouri University of Science and Technology. He is a member of ACI Committees 437 and 440. He has authored and co-authored over 60 refereed journal and conference publications. He was a member of the Task Group that prepared ACI 440.7R-10.

Andrea Prota, ACI Member, is Assistant Professor of Structural Engineering at University of Naples Federico II, Italy. He received his MSc. in Civil Engineering from the Missouri University of Science and Technology and his Ph.D. from the University of Naples Federico II,. His research interests include the use of advanced materials for new construction and retrofitting of structures. He is a member of ACI Committee 440. He was Chair of the Sub-Committee that prepared ACI 440.7R-10.

INTRODUCTION

Unreinforced masonry (URM) structures are prone to extensive damage followed by failure and collapse when subjected to loads resulting from wind, earthquake and other natural or man-made events. Recent earthquakes have clearly demonstrated that the development of effective strategies for the strengthening of masonry is an urgent need. As a response to these challenges, fiber reinforced polymer (FRP) composites may offer technically and economically viable solutions.

The increasing need of FRP materials for the strengthening and upgrade of masonry has motivated the engineering community to produce guides for the proper design, handling and installation of the externally bonded FRP systems. In 2010, the American Concrete Institute (ACI) Committee 440 published "Guide for the Design and Construction of Externally Bonded FRP Systems for Unreinforced Masonry Structures" (ACI 440.7R-10).

RESEARCH SIGNIFICANCE

The development of the design protocols included in ACI 440.7R-10 were, in part, based on calibration of bond reduction factors derived by a database of test results found in the literature. This paper describes the rationale behind this approach, the calibration procedure, and its implementation in design protocols for flexural and shear strengthening of URM walls.

BACKGROUND

FRP Flexural Strengthening

The structural performance of URM walls subject to out-of-plane loading is highly dependent on the tensile strength of masonry and magnitude of the in-plane (axial) compressive forces acting on the wall. URM walls can span in one or two directions depending on the boundary conditions. When subject to out-of-plane loads, initial cracks form at or near the ends of the walls. These cracks are typically located at the base of the wall. After the initial cracking occurs, the wall behaves as a simply-supported element until further cracks develop about mid-height. These cracks typically extend along the mortar bed joints and lead to failure of the wall.

FRP systems can significantly increase the flexural strength of URM walls. Because of the reversed stresses caused by out-of-plane loads due to high wind pressures (windward and leeward) and earthquake excitations, FRP flexural strengthening of URM walls require installation of FRP systems on both wall faces.

FRP composite systems are very effective for strengthening of URM walls that can behave as simply- supported elements, or very nearly so, such as the case of slender walls. FRP composites can also be effective for strengthening of "stocky" walls provided that these are not built between rigid supports (reinforced concrete or steel beams), or that floor or roof structure framing into the wall create a simply-supported boundary conditions (e.g. floor framing consisting of metal deck supported by open-web joists).

Walls with low h/t ratios, typically less than 12, and built between rigid supports can develop arching action. Basically, as a stocky wall bends due to the out-of-plane loads, the wall is restrained from rotation at the supports. This action induces an in-plane compressive force, which depending on the stiffness of the supports can significantly increase the wall resistance to out-of-plane loads. Walls able to develop arching do not typically require to be strengthened, and therefore are not addressed by ACI 440.7R-10.

FRP Shear Strengthening

The structural behavior of URM walls subject to in-plane loads depends on several parameters including geometry such as dimensions and thickness, construction type such as bond pattern, and type and strength of masonry units and mortar; axial loading, and boundary conditions. Walls under in-plane loads can have the following four modes of failure: diagonal tension, bed-joint sliding, toe crushing and rocking. The first three modes of failure are force-controlled failures, whereas rocking is a deformation-controlled failure. Deformation-controlled failures are more ductile than force-controlled failures. A URM wall failing due to rocking (deformation-controlled failure) has the ability to absorb more energy after initial cracking than URM walls failing due to force-controlled failures. Thus, any approach for strengthening of URM walls should be aimed at precluding the occurrence of force-controlled failures, or in its defect it should provide ductility to the wall so this is able to significantly before failure.

FRP composite systems are effective to increase the shear strength of URM walls by preventing or delaying the occurrence of bed-joint sliding failure, if the cracks are oriented along the wall diagonal (i.e. stepped cracking), and diagonal tension failure. FRP composites can also provide pseudo-ductility to URM walls.

There is limited research on infill walls (walls built within reinforced concrete or steel frames) strengthened with FRP; and therefore, strengthening of infill walls is not covered by ACI 440.7R-10. In general the in-plane behavior of infill walls is dependent of the relative stiffness ratio between the masonry and the surrounding frame, aspect ratio of the wall, and occurrence of premature failures such as crushing of corners in contact with the frame.

EFFECTIVE STRAIN IN THE FRP REINFORCEMENT AT ULTIMATE

FRP debonding from the masonry substrate is the most common mode of failure in a URM wall strengthened with FRP systems. Thus, for design purposes, rather than attempting to predict the bond failure, the strain in the FRP laminates can be limited to prevent failure. Since the contribution of FRP to the flexural and shear capacities of the FRP-strengthened is dependant of the strain developed in the FRP, it is reasonable to express the effective strain in the FRP laminate or bar, ε_{fe}, as the product $\kappa_m\varepsilon_{fu}$ for flexural strengthening and $\kappa_v\varepsilon_{fu}$ for shear strengthening, where κ_m and κ_v are bond-dependent coefficients for flexure and shear, respectively, and ε_{fu} is the design rupture strain of FRP.

The methodology to arrive to a set of efficiency coefficients involved collecting test data available in the literature, analyze trends and calibrate appropriate κ_m and κ_v values (Tables 1 through 4). The data base included masonry specimens built with concrete masonry units (CMU), concrete bricks, clay bricks, and strengthened with carbon FRP (CFRP), glass FRP (GFRP) and aramid FRP (AFRP) in the form of externally-bonded laminates or near-surface-mounted (NSM) bars.

Table 1 -- Database for calibration of κ_m – FRP Laminates
(1 in.=25.4 mm, 1 in^2= 645 mm^2, 1 ksi = 6.895 MPa, 1 ft-kips=1.35kN-m)

No.	Source	Specimen	Geometry		Masonry			FRP						Experimental Results	
			h/t	b_m (in)	Type	f'_m (ksi)	t_m (in)	FRP	t_f (in)	A_f (in^2)	f_{fu} (ksi)	E_f (ksi)	ε_{fu} (%)	$M_{exp.}$ (ft-kips)	Failure
1	Hamilton		8.55	24	CMU	2.08	7.75	GFRP	0.014	0.039	220.0	10500	1.50	2.5	Debonding
2	Tumialan	COG3	12.3	24	CMU	1.5	3.75	GFRP	0.014	0.042	220.0	10500	2.1	1.5	Debonding
3	Tumialan	COG3R	12.3	24	CMU	1.5	3.75	GFRP	0.014	0.042	220.0	10500	2.1	2.0	Debonding
4	Tumialan	COG5	12.3	24	CMU	1.5	3.75	GFRP	0.014	0.070	220.0	10500	2.1	2.5	Debonding
5	Tumialan	COG7	12.3	24	CMU	1.5	3.75	GFRP	0.014	0.098	220.0	10500	2.1	2.8	Shear-Debonding
6	Tumialan	COA3	12.3	24	CMU	1.5	3.75	AFRP	0.011	0.033	290.0	17000	1.7	1.9	Debonding
7	Tumialan	COA5	12.3	24	CMU	1.5	3.75	AFRP	0.011	0.055	290.0	17000	1.7	2.6	Debonding
8	Tumialan	CLG3	12.3	24	Clay Brick	2.5	3.75	GFRP	0.014	0.042	220.0	10500	2.1	2.4	Debonding
9	Tumialan	CLG5	12.3	24	Clay Brick	2.5	3.75	GFRP	0.014	0.070	220.0	10500	2.1	3.6	Debonding
10	Tumialan	CLG7	12.3	24	Clay Brick	2.5	3.75	GFRP	0.014	0.098	220.0	10500	2.1	4.9	Debonding
11	Tumialan	CLG7R	12.3	24	Clay Brick	2.5	3.75	GFRP	0.014	0.098	220.0	10500	2.1	5.5	Shear-Debonding
12	Tumialan	CLA3	12.3	24	Clay Brick	2.5	3.75	AFRP	0.011	0.033	290.0	17000	1.7	2.2	Debonding
13	Tumialan	CLA7	12.3	24	Clay Brick	2.5	3.75	AFRP	0.011	0.077	290.0	17000	1.7	4.5	Debonding
14	Tumialan	CLA9	12.3	24	Clay Brick	2.5	3.75	AFRP	0.011	0.099	290.0	17000	1.7	6.2	Rupture
15	Albert	----	19.2	48	CMU	1.06	7.75	GFRP	0.014	0.280	220.0	10500	2.1	15.6	Shear-Debonding
16	Albert	----	18.6	48.2	CMU	1.06	7.75	CFRP	0.007	0.130	372.0	28570	1.3	21.8	Shear-Debonding
17	Albert	----	18.6	48.2	CMU	1.94	7.75	CFRP	0.007	0.130	372.0	28570	1.3	18.1	Shear-Debonding
18	Albert	----	18.6	48.2	CMU	1.94	7.75	CFRP	0.007	0.065	372.0	28570	1.3	9.1	Debonding
19	Hamilton	----	8.55	24	CMU	1.58	7.75	GFRP	0.014	0.039	220.0	10500	2.10	3.1	Rupture
20	Hamilton	----	22.75	24	CMU	2.18	7.75	GFRP	0.014	0.154	220.0	10500	2.10	11.5	Rupture
21	Hamilton	----	8.55	24	CMU	2.08	7.75	GFRP	0.014	0.039	220.0	10500	2.10	3.6	Debonding-Rupture
22	Hamilton	----	8.55	24	CMU	1.58	7.75	GFRP	0.014	0.039	220.0	10500	2.10	4.0	Debonding-Rupture
23	Hamilton	----	22.75	24	CMU	1.98	7.75	GFRP	0.014	0.154	220.0	10500	2.10	14.3	Debonding-Rupture
24	Tumialan	COG5R	12.3	24	Concrete	1.5	3.75	GFRP	0.014	0.070	220.0	10500	2.1	4.0	Shear-Debonding
25	Tumialan	CLA5	12.3	24	Clay Brick	2.5	3.75	AFRP	0.011	0.055	290.0	17000	1.7	3.9	Rupture
26	Tumialan	CLG3R	12.3	24	Clay Brick	2.5	3.75	GFRP	0.014	0.042	220.0	10500	2.1	2.9	Rupture
27	Tumialan	CLG5R	12.3	24	Clay Brick	2.5	3.75	GFRP	0.014	0.070	220.0	10500	2.1	4.0	Rupture

Table 2 -- Database for calibration of κ_m – NSM FRP Bars
(1 in.=25.4 mm, 1 in^2= 645 mm^2, 1 ksi = 6.895 MPa, 1 ft-kips=1.35kN-m)

No.	Source	Specimen	Geometry		Masonry			FRP						Experimental Results	
			h/t	b_m (in)	Type	f'_m (ksi)	t_m (in)	Bar	A_{bar} (in^2)	A_f (in^2)	f_{fu} (ksi)	E_f (ksi)	ε_{fu} (%)	$M_{exp.}$ (ft-kips)	Failure Mode
1	Galati	CO1-GTE1	8.0	24	CMU	1.6	5.75	GFRP Rectangular	0.049	0.049	160.0	6382	2.51	2.47	Debonding
2	Galati	CO1-GTE2	8.0	24	CMU	1.6	5.75	GFRP Rectangular	0.049	0.097	160.0	6382	2.51	5.92	Debonding
3	Galati	CL1-GTE1	12.3	24	Clay Brick	2.3	3.75	GFRP Rectangular	0.049	0.049	160.0	6382	2.51	1.59	Debonding
4	Galati	CL1-GTE2	12.3	24	Clay Brick	2.8	3.75	GFRP Rectangular	0.049	0.097	160.0	6382	2.51	2.70	Debonding
5	Galati	CO2-GRE21	12.7	24	CMU	1.5	3.625	GFRP Round	0.052	0.052	120.0	7276	1.65	1.86	Debonding
6	Galati	CO2-GRE22	12.7	24	CMU	1.5	3.625	GFRP Round	0.052	0.103	120.0	7276	1.65	1.95	Debonding
7	Galati	CO2-GRE21-SJ	12.7	24	CMU	1.5	3.625	GFRP Round	0.052	0.052	120.0	7276	1.65	0.60	Debonding
8	Galati	CO2-GRE22-SJ	12.7	24	CMU	1.5	3.625	GFRP Round	0.052	0.103	120.0	7276	1.65	2.53	Debonding
9	Galati	CO2-GRE21-S	12.7	24	CMU	1.5	3.625	GFRP Round	0.052	0.052	120.0	7276	1.65	1.41	Debonding
10	Tinazzi	Block1	6.0	24	CMU	1.5	7.625	GFRP Round	0.131	0.131	110.0	5920	1.86	2.38	Debonding
11	Tinazzi	Block2	6.0	24	CMU	1.5	7.625	GFRP Round	0.131	0.261	110.0	5920	1.86	5.24	Debonding
12	Tinazzi	Brick1	8.8	5	Clay Brick	2	3.75	GFRP Round	0.052	0.052	120.0	7276	1.65	0.83	Debonding
13	Tinazzi	Brick2	11.5	5	Clay Brick	2	3.75	GFRP Round	0.052	0.052	120.0	7276	1.65	1.20	Debonding
14	Galati	CO2-GRE22-S	12.7	24	CMU	1.5	3.625	GFRP Round	0.052	0.103	120.0	7276	1.65	2.66	Debonding
15	Turco	W3-1	12.7	24	CMU	1.5	3.625	GFRP Round	0.131	0.131	110.0	5920	1.86	1.14	Debonding
16	Turco	W2-2	12.7	24	CMU	1.5	3.625	GFRP Round	0.052	0.103	120.0	7276	1.65	1.23	Debonding
17	Turco	W2-3	12.7	24	CMU	1.5	3.625	GFRP Round	0.052	0.155	120.0	7276	1.65	1.66	Shear-Debonding
18	Bajpai	2 // n	6.0	15.5	CMU	2.2	7.625	GFRP Round	0.052	0.052	115.0	5520	1.95	5.16	Rupture
19	Bajpai	3 // w	6.0	31.4	CMU	2.2	7.625	GFRP Round	0.052	0.155	115.0	5520	1.95	14.26	Rupture
20	Bajpai	4 // w	6.0	31.4	CMU	2.2	7.625	GFRP Round	0.052	0.155	115.0	5520	1.95	14.82	Rupture
21	Bajpai	5 perp n	6.0	15.5	CMU	2.2	7.625	GFRP Round	0.052	0.052	115.0	5520	1.95	5.69	Rupture
22	Bajpai	6 perp n	6.0	15.5	CMU	2.2	7.625	GFRP Round	0.052	0.052	115.0	5520	1.95	5.35	Rupture
23	Bajpai	7 perp w	6.0	31.4	CMU	2.2	7.625	GFRP Round	0.052	0.155	115.0	5520	1.95	14.44	Rupture
24	Bajpai	8 perp w	6.0	31.4	CMU	2.2	7.625	GFRP Round	0.052	0.155	115.0	5520	1.95	14.89	Rupture

Table 3 -- Database for calibration of κ_v – FRP Laminates
(1 in.=25.4 mm, 1 in^2= 645 mm^2, 1 ksi = 6.895 MPa, 1 kip=4.448 kN)

No.	Source	Specimen	MASONRY					FRP					Experimental Results	
			Type	h (in)	d (in)	tm (in)	f'm (psi)	FRP	f_{fu} (ksi)	Ef (ksi)	εfu (%)	Af (in^2)	$V_{exp.}$ (kips)	Failure Mode
1	Grando	GL-4	CMU	64	64	5.625	2430	GFRP	220	10000	2.20	21.0	46.8	Diagonal Shear
2	Grando	CL-1	CMU	64	64	5.625	2430	CFRP	500	33000	1.52	14.0	25.4	Diagonal Shear
3	Morbin	GL-1	CMU	64	64	5.625	2430	GFRP	220	10000	2.20	16.0	42.0	Diagonal Shear
4	Santa Maria	FX-01	Clay Brick	80	80	5.6	1595	CFRP	500	33000	1.52	24.0	58.3	Diagonal Shear
5	Santa Maria	FX-02	Clay Brick	80	80	5.6	1595	CFRP	500	33000	1.52	16.0	51.6	Diagonal Shear
6	Santa Maria	FH-02	Clay Brick	80	80	5.6	1595	CFRP	500	33000	1.52	36.0	51.0	Diagonal Shear
7	Santa Maria	FH-04	Clay Brick	80	80	5.6	1595	CFRP	500	33000	1.52	24.0	49.5	Diagonal Shear
8	Senescu	Single W	Clay Brick	30	30	3.625	2906	GFRP	44.1	2270	1.94	30.0	56.0	Diagonal Shear
9	Stratford	Conc2	Conc. Brick	48	48	4	1500	GFRP	143	10633	1.34	48.0	24.7	Diagonal Shear
10	Stratford	Conc3	Conc. Brick	48	48	4	1500	GFRP	143	10633	1.34	48.0	27.0	Diagonal Shear
11	Valluzzi	PR1Carb2F	Clay Brick	20.4	20.4	4.8	806	CFRP	500	33000	1.52	2.8	22.6	Diagonal Shear
12	Valluzzi	PR2Carb2F	Clay Brick	20.4	20.4	4.8	806	CFRP	500	33000	1.52	2.8	25.5	Diagonal Shear
13	Valluzzi	PR3Carb2F	Clay Brick	20.4	20.4	4.8	806	CFRP	500	33000	1.52	2.8	22.6	Diagonal Shear
14	Valluzzi	PR1Glass2F	Clay Brick	20.4	20.4	4.8	806	GFRP	240	9400	2.55	7.1	24.0	Diagonal Shear
15	Valluzzi	PR2Glass2F	Clay Brick	20.4	20.4	4.8	806	GFRP	240	9400	2.55	7.1	30.4	Diagonal Shear
16	Valluzzi	PR3Glass2F	Clay Brick	20.4	20.4	4.8	806	GFRP	240	9400	2.55	7.1	23.2	Diagonal Shear
17	Valluzzi	PRD1Carb2F	Clay Brick	20.4	20.4	4.8	806	CFRP	500	33000	1.52	4.0	32.2	Diagonal Shear
18	Valluzzi	PRD2Carb2F	Clay Brick	20.4	20.4	4.8	806	CFRP	500	33000	1.52	4.0	33.6	Diagonal Shear
19	Valluzzi	PRD1Glass2F	Clay Brick	20.4	20.4	4.8	806	GFRP	240	9400	2.55	6.6	38.3	Diagonal Shear
20	Valluzzi	PRD2Glass2F	Clay Brick	20.4	20.4	4.8	806	GFRP	240	9400	2.55	6.6	40.5	Diagonal Shear
21	Zhao	Wall2	Clay Brick	39.4	55.1	9.4	980	CFRP	300	20000	1.50	11.8	74.6	Diagonal Shear
22	Zhao	Wall3	Clay Brick	39.4	55.1	9.4	980	CFRP	300	20000	1.50	11.8	75.5	Diagonal Shear
23	Zhao	Wall4	Clay Brick	39.4	55.1	9.4	980	CFRP	300	20000	1.50	7.9	64.7	Diagonal Shear
24	Tinazzi	Wall 5	Clay Brick	24	24	3.625	2050	GFRP	220	10500	2.10	32.0	26.1	Diagonal Shear
25	Tinazzi	Wall 6	Clay Brick	24	24	3.625	2500	GFRP	220	10500	2.10	16.0	28.7	Diagonal Shear
26	Santa Maria 1	MDF2	Clay Brick	44	42.4	5.6	1494	CFRP	500	33000	1.51515	24.0	44.0647	Diagonal Shear
27	Santa Maria 1	MDF3	Clay Brick	44	42.4	5.6	1494	CFRP	500	33000	1.51515	24.0	44.0647	Diagonal Shear
28	Santa Maria 1	CDF4	Clay Brick	44	42.4	5.6	1494	CFRP	500	33000	1.51515	24.0	45.1888	Diagonal Shear
29	Santa Maria 1	CDF5	Clay Brick	44	42.4	5.6	1494	CFRP	500	33000	1.51515	24.0	45.6385	Diagonal Shear
30	Santa Maria 1	MHL2	Clay Brick	44	42.4	5.6	1494	CFRP	406	23200	1.75	12.0	31.9245	Diagonal Shear
31	Santa Maria 1	CHL3	Clay Brick	44	42.4	5.6	1494	CFRP	406	23200	1.75	12.0	34.6223	Diagonal Shear
32	Santa Maria 1	CHL4	Clay Brick	44	42.4	5.6	1494	CFRP	406	23200	1.75	12.0	32.8237	Diagonal Shear
33	Santa Maria 1	MHF3	Clay Brick	44	42.4	5.6	1494	CFRP	500	33000	1.51515	12.0	35.2968	Diagonal Shear
34	Santa Maria 1	CHF4	Clay Brick	44	42.4	5.6	1494	CFRP	500	33000	1.51515	12.0	40.2428	Diagonal Shear
35	Santa Maria 1	CHF5	Clay Brick	44	42.4	5.6	1494	CFRP	500	33000	1.51515	12.0	43.6151	Diagonal Shear

Table 4 -- Database for calibration of κ_v – NSM FRP Bars
(1 in.=25.4 mm, 1 in^2= 645 mm^2, 1 ksi = 6.895 MPa, 1 kip=4.448 kN)

No.	Source	Specimen	MASONRY					FRP						Experimental Results	
			Type	h (in)	d (in)	tm (in)	f'm (psi)	FRP	f_{fu} (ksi)	Ef (ksi)	εfu (%)	Abar (in^2)	Af (in^2)	$V_{exp.}$ (kips)	Failure Mode
1	Grando	COW2	CMU	64	64	5.625	2430	GFRP Round	120	7276	1.65	0.05	0.350	31.8	Diagonal Shear
2	Grando	COW3	CMU	64	64	5.625	2430	GFRP Round	120	7276	1.65	0.05	0.350	31	Diagonal Shear
3	Grando	COW8	CMU	64	64	5.625	2430	GFRP Round	120	7276	1.65	0.05	0.350	29.3	Diagonal Shear
4	Grando	CT-3	CMU	64	64	5.625	2430	CFRP Rectangular	201.9	20702	0.98	0.05	0.144	30.0	Diagonal Shear
5	Grando	CT-5	CMU	64	64	5.625	2430	CFRP Rectangular	201.9	20702	0.98	0.05	0.240	24.4	Diagonal Shear
6	Morbin	COW10	CMU	64	64	5.625	2430	GFRP Round	120	7276	1.65	0.05	0.350	38.3	Diagonal Shear
7	Morbin	COW12	CMU	64	64	5.625	2430	GFRP Round	120	7276	1.65	0.05	0.150	30.3	Diagonal Shear
8	Secondin	GT-3	CMU	64	64	5.625	2430	GFRP Rectangular	160	6382	2.51	0.05	0.146	35.4	Diagonal Shear
9	Secondin	GT-5	CMU	64	64	5.625	2430	GFRP Rectangular	160	6382	2.51	0.05	0.243	39.4	Diagonal Shear
10	Tinazzi	Wall2	Clay Brick	24	24	3.625	2500	GFRP Round	120	5920	2.027	0.05	0.400	25.2	Diagonal Shear
11	Tinazzi	Wall3	Clay Brick	24	24	3.625	2500	GFRP Round	120	5920	2.027	0.05	0.400	20.8	Diagonal Shear
12	Tinazzi	Wall4	Clay Brick	24	24	3.625	2500	GFRP Round	120	5920	2.027	0.05	0.400	23.3	Diagonal Shear
13	Tinazzi	Wall7	Clay Brick	24	24	3.625	2050	GFRP Round	120	5920	2.027	0.05	0.800	28.0	Diagonal Shear
14	Tinazzi	Wall10	Clay Brick	24	24	7.25	2050	GFRP Round	120	5920	2.027	0.05	0.800	21.5	Diagonal Shear
15	Tumialan	W2	CMU	64	64	5.625	2430	GFRP Round	120	7276	1.65	0.05	0.350	51.3	Diagonal Shear
16	Tumialan	W3	CMU	64	64	5.625	2430	GFRP Round	120	7276	1.65	0.05	0.500	56.3	Diagonal Shear
17	Tumialan	W4	CMU	64	64	5.625	2430	GFRP Round	120	7276	1.65	0.05	0.500	53.8	Diagonal Shear
18	Yu	W3	CMU	64	64	5.625	2430	GFRP Round	120	7276	1.65	0.05	0.150	29.8	Diagonal Shear
19	Yu	W4	CMU	64	64	5.625	2430	GFRP Round	120	7276	1.65	0.05	0.350	35.6	Diagonal Shear

Effective strain for flexure-controlled sections

The effective strain and stress used for the design of the flexural strengthening of URM walls due to out-of-plane and in-plane loads is limited to the strain level at which debonding may occur, ε_{fd}:

$$\varepsilon_{fd} = \kappa_m \varepsilon_{fu}^* \leq C_E \varepsilon_{fu}^* \qquad \text{ACI 440.7R Eq. (8-6)}$$

ε_{fu}^* is the ultimate rupture strain of the FRP reinforcement as reported by the manufacturer and C_E is an environmental reduction factor, which depends on the FRP system and exposure condition (ACI 440.7R Table 8.1)

Where the κ_m coefficients are set as:

$$\kappa_m = \begin{cases} 0.45 \text{ for surface–mounted FRP systems} \\ 0.35 \text{ for NSM FRP systems} \end{cases} \qquad \text{ACI 440.7R Eq. (8-8)}$$

It should be noted that surface-mounted FRP systems include wet layup or precured systems (hereafter referred to as laminates). Also, Eq. (8-8) is applicable only when the total force per unit width (per bar for NSM systems) that the FRP system transfers to the masonry substrate satisfies the limitation given in Eq. (8-9).

$$\rho_{fm} = \begin{cases} n t_f f_{fe} \leq 1500 \text{ lb/in. for surface–mounted FRP systems} \\ A_{f,bar} \leq 10{,}000 \text{ lb/bar for NSM FRP systems} \end{cases} \qquad \text{ACI 440.7R Eq. (8-9)}$$

(1 lb/in= 0.175 N/mm, 1 lb= 4.448 N)

Basis for bond-reduction coefficient for flexure (κ_m) – Previous investigations show that URM walls strengthened in flexure with FRP systems have the following modes of failure: 1) debonding of the FRP laminate or bar from the masonry substrate; 2) flexural failure (i.e. rupture of the FRP laminate in tension or crushing of the masonry in compression); and, 3) shear failure in the masonry. Of these three modes of failure, debonding is the most common mode of failure

The majority of the test results used in the data base did not report the strain in FRP at failure (experimental effective strain). Thus, the data analysis required back-calculations to estimate the effective strain, using the moment at failure, and strain compatibility and internal force equilibrium principles. Similarly to the analysis of concrete members strengthened with FRP, well-established relationships were used to define the masonry compressive block equivalent to the non-linear stress-strain distribution. In accordance with MSJC recommendations, the maximum usable strain ε_{mu} was 0.0035 in./in. (mm/mm) for clay masonry, and 0.0025 in./in. (mm/mm) for concrete masonry. The tensile strength of masonry was neglected. For data points reporting experimental strains, the back-calculation procedure showed good agreement between the experimental and analytical strains.

The bond-reduction coefficient, κ_m, is basically an efficiency factor, measured as the ratio between the effective strain in the FRP and the ultimate tensile strain of FRP. Figures 1a and 1b illustrate the relationship between the effective-to-ultimate strain ratio, $\varepsilon_{fe}/\varepsilon_{fu}$, and the adjusted reinforcement ratio, ω_f, for masonry specimens strengthened with FRP laminates and FRP bars, respectively. The term ω_f is expressed as: $\rho_f E_f / f'_m (h/t)$, where: ρ_f is the FRP reinforcement ratio equal to $A_f/(b\ t)$ (FRP area over cross-section area), E_f is the FRP elastic modulus, f'_m is the masonry compressive strength, and h/t is the wall height-to-thickness slenderness ratio. The ω_f ratio intends to capture the effect of other parameters, in addition to ρ_f, influencing the wall behavior: 1) the FRP stiffness; 2) the masonry compressive strength that directly affects the out-of-plane flexural capacity; and, 3) the slenderness ratio h/t that is identified as one of the most influential parameters in the out-of-plane behavior of masonry walls. The slenderness ratio and the out-of-plane capacity are inversely proportional: as the slenderness ratio decreases, the out-of-plane flexural capacity becomes larger.

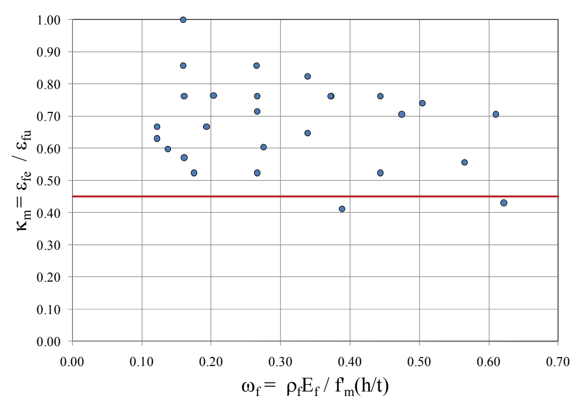

(a) FRP Laminates

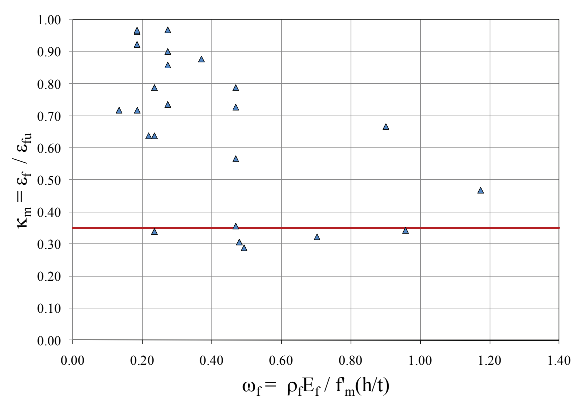

(b) NSM FRP Bars

Figure 1 – κ_m vs. ω_f Plots

Figures 1a and 1b do not show a clear trend that can be used to establish an equation or set of equations to compute κ_m. However, the diagrams suggest that the lower limits of κ_m for masonry strengthened with FRP laminates can be taken as 0.45; whereas for masonry strengthened with FRP bars, this value can be taken as 0.35. Figure 2a and 2b show the correlation between the experimental and expected flexural strengths.

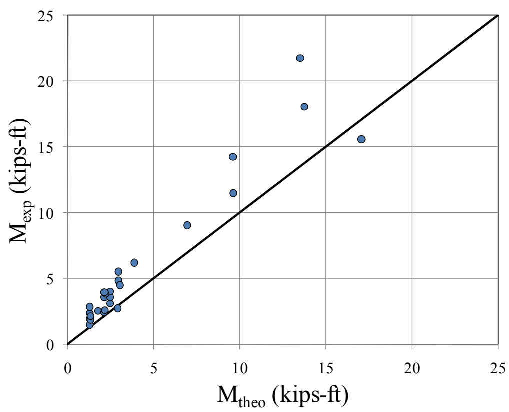

(a) FRP Laminates

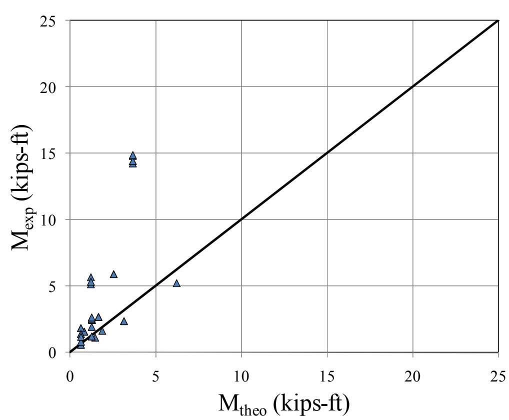

(b) NSM FRP Bars

Figure 2 – Validation of Design Approach for Flexural Strengthening

It is important to note that the database represents research on a fairly limited range of FRP system types and layouts. The FRP systems tested involve the use of commercially available FRP fabric systems or NSM bars. However most only use one layer of FRP fabric or small diameter (1/2 in. [25 mm] or less) bars. Due to the limited range of FRP systems tested, it is not currently known how the use of much higher stiffness systems (such as multiple layer systems or large diameter bars) would affect the effective strain. It would be expected that higher stiffness systems would result in lower effective strains. However, the extent to which the strain would be reduced is not known at this time. It is for this reason that the limitations given in Eq. (8-9) are introduced. These criteria limit the type of FRP system used to the range of systems that are in the current database.

Effective strain for shear-controlled sections

The effective strain and stress used for the design of the shear strengthening of URM walls due to in-plane loads is limited to the strain level at which premature failures may occur, ε_{fd}:

$$\varepsilon_{fd} = \kappa_v \varepsilon_{fu}^{*} \leq C_E \varepsilon_{fu}^{*} \qquad \text{ACI 440.7R Eq. (8-10)}$$

The κ_v coefficient depends on the FRP reinforcement index ω_f, as defined in the following equation:

$$\omega_f = \frac{1}{1000} \frac{A_f E_f}{A_n \sqrt{f_m'}} \quad \text{(in-lbs units)} \qquad \text{ACI 440.7R Eq. (8-12)}$$

Where the κ_v coefficients are defined as follows:

$$\kappa_v = \begin{cases} 0.40 \text{ for } \omega_f \leq 0.20 \\ 0.64 - 1.2\omega_f \text{ for } 0.20 < \omega_f \leq 0.45 \\ 0.10 \text{ for } \omega_f > 0.45 \end{cases} \qquad \text{ACI 440.7R Eq. (8-13)}$$

Similar to flexure-controlled failure modes, Eq. (8-13) is applicable only when the force per unit width (per bar for NSM systems) that the FRP system transfers to the masonry substrate satisfies the limitation given in Eq. (8-14).

$$\rho_{fm} = \begin{cases} n t_f f_{fe} \leq 1500 \text{ lb/in. for surface-mounted FRP systems} \\ A_{f,bar} \leq 10{,}000 \text{ lb/bar for NSM FRP systems} \end{cases} \qquad \text{ACI 440.7R Eq. (8-14)}$$

(1 lb/in= 0.175 N/mm, 1 lb= 4.448 N)

It is recognized that the κ_m and κ_v coefficients in Eq. (8-6) and Eq. (8-10) will always control over the C_E coefficients. However it should be noted that the bond dependent coefficients were set as a lower bound based on available experimental data. Future investigations may provide in higher κ_m and κ_v coefficients. The upper limitation involving the C_E factor is included to establish a design philosophy that will remain consistent. Furthermore, ACI 440.7R recommends the use of larger values of κ_m and κ_v for a particular application is available, if these coefficients are properly substantiated by testing.

Basis for bond-reduction coefficient for shear (κ_v) – In walls strengthened with FRP, shear failure develops from an initial diagonal crack, which is followed by secondary cracks, typically parallel to the first crack. Diagonal cracks run through masonry units (common in brick walls) or can follow the mortar joints – stepped cracking (common in CMU walls). As the cracks in the wall grow and widen, the wall fails when the FRP system debonds from the masonry substrate and/or when the masonry is unable to transfer shear friction through cracked interfaces because of the wide cracks.

The bond-reduction coefficient κ_v accounts for the premature failure of the FRP-strengthened wall caused by these mechanisms. For the data analysis the coefficient κ_v was estimated as the ratio between the experimental shear contribution of FRP, $V_{f\text{-}exp}$, and the expected maximum shear contribution of FRP, V_{fmax}, to the overall wall shear capacity if premature failures do not occur (i.e. FRP rupture governs the wall behavior). V_{fexp} was determined by subtracting the ultimate load reported for the control walls (unstrengthened walls) from the ultimate loads of the strengthened walls. V_{ftheo} was estimated using the following equation:

$$V_{ftheo} = \kappa_v \frac{A_f f_{fu} d_v}{s_f} \cos\alpha \qquad \text{Eq. (1)}$$

A_f is the total area of FRP reinforcement, f_{fu} is the ultimate FRP tensile strength, d_v is the actual depth of masonry in direction of the shear force, s_f is the center-to-center spacing between each FRP laminate or bar, and α represents the fibers inclination.

Figures 3a and 3b illustrate the relationship between ratio of the experimental and theoretical FRP shear contribution and the adjusted reinforcement ratio, ω_{fv}, for masonry specimens strengthened with FRP laminates and FRP bars, respectively. ω_{fv} intends to recognize the relationship between the FRP stiffness and the masonry shear strength, and it is expressed as:

$$\omega_{fv} = \frac{A_f E_f}{A_m \sqrt{f'_m}} \quad \text{(in-lbs units)} \qquad \text{Eq. (2)}$$

Where: E_f is the FRP elastic modulus, A_m is the net shear area, and f'_m is the masonry compressive strength.

Although, the diagrams do not show a clear trend, two zones for κ_v can be distinguished. This suggests that κ_v can be defined based on the magnitude of the reinforcement ratio ω_{fv}. Basically, larger κ_v coefficients are observed when ω_{fv} are about or smaller than 0.20. The κ_v coefficients decrease to about 0.10 when ω_{fv} are larger than 0.45. Figures 4a and 4b show the correlation between the experimental and expected shear strengths.

Similar to Eq. (8-9) for flexure-controlled sections, Eq. (8-14) provides criteria that limit the type of FRP systems used to the range of systems that are in the current database.

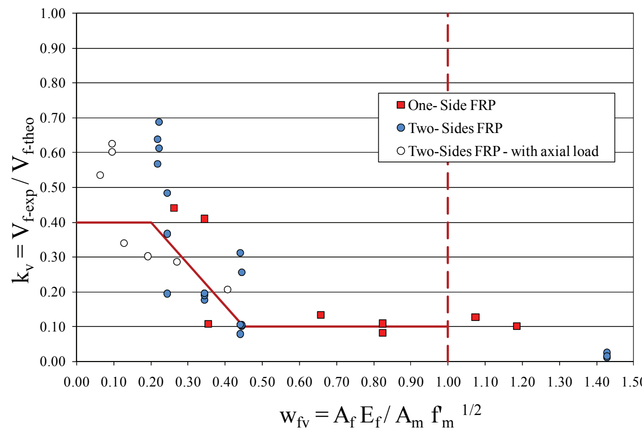

(a) FRP Laminates

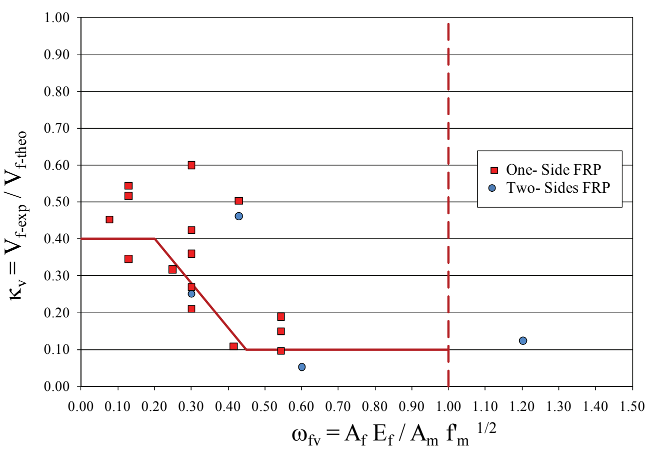

(b) NSM FRP Bars

Figure 3 – κ_v vs. ω_f Plots

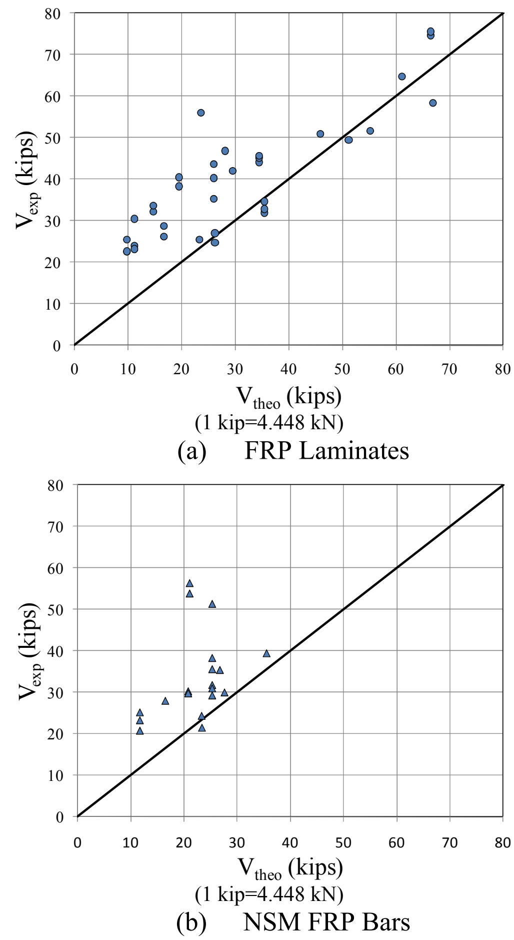

Figure 4 – Validation of Design Approach for Shear Strengthening

DESIGN PROTOCOLS FOR FRP STRENGTHENING OF URM WALLS

FRP Flexural strengthening for out-of-plane loads

Nominal Flexural Strength – The ultimate strength design method requires that the design flexural strength of the strengthened wall must exceed the flexural demand:

$$\phi M_n \geq M_u \qquad \text{ACI 440.7R Eq. (9-1)}$$

The nominal flexural capacity is computed considering a reduction factor, ϕ, equal to 0.60, which is similar to the ϕ-factor specified by the Building Code Requirements and Specification for Masonry Structures (MSJC 2008) for URM walls subjected to flexural loads, axial loads or combination of both. The use of this ϕ-factor is justified by the need to compensate a section with low ductility with a higher reserve of strength. The approach for the reduction factor is similar to that of the ACI-318, where a section with low ductility must be compensated with a higher reserve of strength. The higher reserve of strength can be attained by applying a strength reduction factor of 0.60 to sections prone to have brittle or premature failures such as debonding of the FRP laminate.

The nominal flexural strength M_n of an FRP-strengthened URM wall is expressed as shown in the equation below. In this equation the factored axial load, Pu, is assumed to be acting at the wall section centroid. The equation can be modified to include the effect of the eccentric loads, typically found in load-bearing masonry construction.

$$M_n = A_f f_{fe}\left(d_f - \frac{\beta_1 c}{2}\right) + P_u\left(\frac{t}{2} - \frac{\beta_1 c}{2}\right) \qquad \text{ACI 440.7R Eq. (9-2)}$$

The maximum strain level that can be achieved in the FRP reinforcement will be governed by either the strain level developed in the FRP at the point at which masonry crushes, or the point at which the FRP debonds from the substrate. The effective strain level in the FRP reinforcement at ultimate limit can be calculated from the following relationship.

$$\varepsilon_{fe} = \varepsilon_{mu}\left(\frac{t-c}{c}\right) \le \min\left(\kappa_m \varepsilon_{fu}^*, C_E \varepsilon_{fu}^*\right) \qquad \text{ACI 440.7R Eq. (9-3)}$$

The flexural strength is calculated by solving Eq. 9-2 and Eq. 9-3, including the parameters defining the well-known rectangular stress block in the masonry equivalent the nonlinear distribution of stress, and considering the following assumptions:

- The strains in the FRP reinforcement and masonry are directly proportional to their distance from the neutral axis
- The maximum usable compressive strain in concrete masonry is 0.0025, and 0.0035 for clay and natural stone masonry
- FRP reinforcement is linear elastic up to failure
- The contributions of masonry in tension and FRP reinforcement in compression are neglected
- There is no relative slip between the FRP reinforcement and masonry until debonding failure occurs; and
- The wall behaves as a simply supported element or very nearly so (i.e. arching mechanism does not develop)

Limitations for FRP Flexural Strengthening – There are two primary limitations for strengthening of URM walls with FRP, related to the slenderness ratio h/t of the wall.

- Walls with h/t larger than 20 should not be strengthened with FRP systems unless the efficiency of FRP has been properly substantiated by testing. This limitation is based on the h/t ratios included limitation in the database used to calibrate the bond-dependent coefficient, and in the risk of strengthening very slender walls which could potentially be unstable due to out-of-plane load and secondary bending moments caused by axial loads (including self-weight) when deforming due to the out-of-plane loading.

- Walls with h/t smaller than 8 and built within stiff supports most likely will not require to be strengthened because the wall can develop arching mechanism. Galati et al. (2007) presents a protocol for FRP flexural strengthening of URM walls in the event that the analysis considering arching shows that strengthening is required. It should be noted that the contribution of FRP to the URM flexural strength is not as pronounced as in the cases of slender and/or simply-supported walls, being many times just a marginal increase.

FRP Spacing Limits in Flexural Strengthening – ACI 440.7R recommends that the maximum center-to-center spacing of FRP systems in walls strengthened in flexure should meet the following spacing requirements.

FRP laminates: $s_{f,max} \le 3t + w_f$

NSM FRP bars: $s_{f,max} \le 3t$

Where w_f is the width of the FRP laminate

These reduced limits are conservative design considerations, which are justified by the difference in behavior between an FRP-strengthened URM wall and a reinforced wall with steel reinforcement in grouted cells. In a new reinforced masonry wall, in addition to span between supports, masonry also spans between the grouted cells, which essentially behave as pilasters. For this reason the steel reinforcement can be spaced up to 6t. Contrarily, in an FRP-strengthened URM wall, the FRP reinforcement is not grouted and the FRP sections are not stiff enough to cause horizontal bending.

FRP shear strengthening for in-plane loads

Nominal Shear Strength – The ultimate strength design method requires that the design shear strength of the strengthened wall must exceed the shear demand:

$$\phi V_n \ge V_u \qquad \text{ACI 440.7R Eq. (10-2)}$$

The nominal shear capacity is computed considering a reduction factor, ϕ, equal to 0.80, which is similar to the ϕ-factor specified by MSJC (2008) for URM walls subjected to shear loads.

The nominal shear strength V_n of the FRP-strengthened wall can be estimated as the summation of the contributions of masonry and FRP.

$$V_n = V_n^{URM} + V_f \qquad \text{ACI 440.7R Eq. (10-3)}$$

V_n^{URM} is the nominal shear strength given of the unreinforced wall, which can be estimated following recommendations provided by MSJC or ASCE-41 (2006). The FRP contribution to the shear strength V_f can be estimated as:

$$V_f = \begin{cases} p_{fv} w_f \dfrac{d_v}{s_f} \text{ for surface-mounted FRP systems} \\ p_{fv} \dfrac{d_v}{s_f} \text{ for NSM FRP systems} \end{cases}$$ ACI 440.7R Eq. (10-4)

Where p_{fv} is computed according to Eq. 8-14, w_f is the width of the FRP laminates, s_f is the center-to-center spacing between strips or bars, and dv is the effective masonry depth for shear calculations, calculated as the minimum of the wall height H, and the wall length L.

Limitations for FRP Shear Strengthening – The in-plane shear performance of FRP-strengthened walls depends on the type of masonry construction and the FRP strengthening layout. Test results have shown that FRP systems can significantly increase the shear capacity of URM walls when the existing shear strength of the wall is not large such as the case of single-wythe or ungrouted walls). Contrarily, when the existing shear strength of the URM wall is large (multi-wythe or grouted walls), the contribution of FRP has been marginal in some situations. Test results also indicate that the FRP layout influences the structural performance of the wall. For instance, in thick walls, FRP placed on the two wall sides has been shown to be more effective than FRP placed on one side. In the absence of project specific experimental evidence, ACI 440.7R-10 recommends adopting the limitations shown on Table 5.

Table 5 -- FRP limitations for shear strengthening (ACI 440.7R Table 10.1)

Masonry Type	Wall Construction	FRP Strengthening Layout
Hollow unit masonry wall	t = 8 in. (200 mm) or less Ungrouted or partially grouted walls with grouted cells spaced greater than 48 in. (1.20 m)	FRP on one face of wall is acceptable
	t = 8 in. (200 mm) or less Fully or partially grouted walls with grouted cells spaced at 48 in. (1.20 m) or less	FRP on two faces of wall is required
	t = 10 to 12 in. (250 to 300 mm) Ungrouted or partially grouted walls with grouted cells spaced greater than 60 in. (1.50 m)	FRP on two faces of wall is required
	t = 10 to 12 in. (250 to 300 mm) Fully or partially grouted walls with grouted cells spaced at 60 in. (1.50 m) or less	Use of FRP is not recommended
	t greater than 12 in. (300 mm) Ungrouted or grouted	Use of FRP is not recommended
Solid unit masonry wall	Single-wythe walls with t = 4 in. (100 mm) or less	FRP on one face of wall is acceptable
	Double-wythe walls with t = 8 in. (200 mm) or less	FRP on two faces of wall is required
	Multi-wythe walls with t > 8 in. (200 mm)	Use of FRP is not recommended

FRP Spacing Limits in Shear Strengthening – ACI 440.7R recommends that that the maximum center-to-center spacing of FRP systems in walls strengthened in shear should meet the following requirements.

FRP laminates: $s_{f,max} \leq 16\text{ in.}(400\text{ mm}) + w_f$

NSM FRP bars: $s_{f,max} \leq 16\text{ in.}(400\text{ mm})$

The spacing limitation of 16 in. (400 mm) is based on MSJC provisions for spacing of horizontal reinforcement when the reinforcement is placed in the bed joints.

FINAL REMARKS

The retrofitting of existing masonry with FRP systems is of particular relevance for the case of URM walls to improve capacity under out-of-plane and in-plane loads. It is expected that the use of FRP systems in masonry applications will become a more common staple for design professionals and contractors with the availability of ACI guides for design and construction procedures of masonry strengthening with FRP systems.

REFERENCES

American Concrete Institute - Committee 440, (2010), "Guide for the Design and Construction of Externally Bonded FRP Systems for Unreinforced Masonry Structures," ACI 440.7R-10.

Albert, L. M.; Elwi, A. E.; and Cheng, J. J., 2001, "Strengthening of Unreinforced Masonry Walls Using FRPs," Journal of Composites for Construction, ASCE, V. 5, No. 2, pp. 76-84.

Bajpai, K., and Duthinh, D., 2003, "Flexural Strengthening of Masonry Walls with External Composite Bars," The Masonry Society Journal, V. 21, No. 1, pp. 9-20.

Galati, N., T. Hrynyk, J.G. Tumialan, G. R. Bell, J.J. Myers, and A. Nanni, "A Simplified Design Methodology Accounting for the Arching Effects in Masonry Walls Strengthened with FRP Materials and Subject to Out-of-Plane Loads," 10th North American Conference (10NAMC), June 3-6, 2007, St. Louis, MO, pp. 299-310.

Grando, S.; Valluzzi, M. R.; Tumialan, J. G.; and Nanni, A., 2003, "Shear Strengthening of URM Clay Walls with FRP Systems," Proceedings of the International Symposium FRPRCS-6, Singapore, V. 2, pp. 1229-1238.

Hamilton III, H. R., and Dolan, C. W., 2001, "Flexural Capacity of Glass FRP Strengthened Concrete Masonry Walls," Journal of Composites for Construction, V. 5, No. 3, pp. 170-178.

Masonry Standards Joint Committee (MSJC), 2008, "Building Code Requirements and Specification for Masonry Structures," American Concrete Institute, Farmington Hills, MI.

Santa Maria, H.; Duarte, G.; and Garib, A., 2004, "Experimental Investigation of Masonry Panels Externally Strengthened with CFRP Laminates and Fabric Subjected to In-Plane Shear Load," 13th Word Conference on Earthquake Engineering, Vancouver, BC, Canada, 10 pp.

Santa Maria, H.; Alcaino, P.; and Luders, C., 2006, "Experimental Response of Masonry Walls Externally Reinforced with Carbon Fiber Fabrics," Paper No. 1402, 8th U.S. National Conference on Earthquake Engineering, San Francisco, CA, 10 pp.

Tinazzi, D., and Nanni, A., 2000, "Assessment of Technologies of Masonry Retrofitted with FRP," Report No. CIES 00-18, Center for Infrastructure Engineering Studies, University of Missouri-Rolla, Rolla, MO, 148 pp.

Tumialan, J. G.; Morbin, A., Nanni A.; and Modena, C., 2001a, "Shear Strengthening of Masonry Walls with FRP Composites," COMPOSITES 2001 Convention and Trade Show, Composites Fabricators Association, Tampa, FL, Oct. 3-6, 6 pp. (CD-ROM)

Tumialan, J. G.; Galati, N.; and Nanni, A., 2003b, "Fiber-Reinforced Polymer Strengthening of Unreinforced Masonry Walls Subject to Out-of-Plane Loads," ACI Structural Journal, V. 100, No. 3, May-June, pp. 321-329.

Turco, V.; Galati, N.; Tumialan, J. G.; and Nanni, A., 2003, "Flexural Strengthening of URM Walls with FRP Systems," Proceedings of the Sixth International Symposium on FRP Reinforcement for Concrete Structures (FRPRCS-6), Singapore, pp. 1219-1228.

Valluzzi, M. R.; Tinazzi, D.; and Modena, C., 2002, "Shear Behavior of Masonry Panels Strengthened by FRP Laminates," Construction and Building Materials, V. 16, No. 7, pp. 409-416.

Zhao, T.; Zhang, C. J.; and Xie, J., 2003, "Experimental Study on Earthquake Strengthening of Brick Walls with Continuous Carbon Fibre Sheet," Masonry International, V. 16, No. 1, pp. 21-25.